2015 International Symposium on Nonlinear Theory and its Applications
NOLTA2015, Kowloon, Hong Kong, China, December 1-4, 2015

Symmetry and Dynamics of a Coupled Gyroscope System

Pietro-Luciano Buono†, Bernard S. Chan‡, Antonio Palacios‡ and Visarath In§

†Faculty of Science, University of Ontario Institute of Technology
2000 Simcoe St N, Oshawa, ON L1H 7K4, Canada
‡Nonlinear Dynamical Systems Group, Department of Mathematics,
San Diego State University, San Diego, CA 92182, USA
§Space and Naval Warfare Systems Center, Code 71730
53560 Hull Street, San Diego, CA 92152-5001, USA
Email: Pietro-Luciano.Buono@uoit.ca, bchan@mail.sdsu.edu, apalacios@mail.sdsu, visarath@spawar.navy.mil

Abstract—Traditional gyroscopes are mechanical devices used for measuring and maintaining orientation. They consist of spinning discs enclosed in gimbal rings that allowed for free rotation in any orientation. New manufacturing techniques in microelectromechanical systems (MEMS) allow for mass manufacturing of low-cost and miniaturized vibratory gyroscopes. At the same time, these smaller gyroscopes are more prone to external perturbations. Small disturbances, such as thermo interference, can increase phase drifts in the oscillatory signal and give inaccurate results, specially for guidance systems. To remedy the lowered sensitivity problem, we consider networks of coupled MEMS gyroscopes. We apply group theoretical methods and normal form techniques to simplify the governing equations. Analysis of the normal form equations allows us to unravel the nature of the bifurcations that lead a ring of gyroscopes of any size into and out of synchronization. From an engineering standpoint, the synchronization regime is of particular importance because it can lead to a significant reduction in phase drift.

1. Introduction

High-dimensional nonlinear systems with symmetry arise naturally at various length scales: in molecular dynamics [1], underwater vehicle dynamics [2], in magnetic- and electric-field sensors [3, 4, 5], in gyroscopic [6, 7] and navigational systems [8, 9], hydroelastic rotating systems and boats/ships [10, 7], and in *complex systems* such as telecommunication infrastructures [11] and power grids [12]. Whereas the theory of symmetry breaking bifurcations of typical invariant sets, i.e., equilibria, periodic solutions, and chaos, is well-developed for general low-dimensional systems [13], there are significantly fewer results on the corresponding theory for symmetric high-dimensional nonlinear *mechanical and electrical* systems, including coupled Hamiltonian systems [14, 15]. Consequently, the aim of this work is to advance the study of the role of symmetry in high-dimensional nonlinear systems with Hamiltonian structure. As a case study, we consider a network of vibratory gyroscopes coupled bidirectionally in a ring.

A conventional vibratory gyroscope consists of a proof-mass system as is shown in Fig. 1. The system operates [16, 17, 18] on the basis of energy transferred from a driving mode to a sensing mode through the Coriolis force. In this configuration, a change in the acceleration around the driving x-axis caused by the presence of the Coriolis force induces a vibration in the sensing y-axis which can be converted to measure angular rate output or absolute angles of rotation.

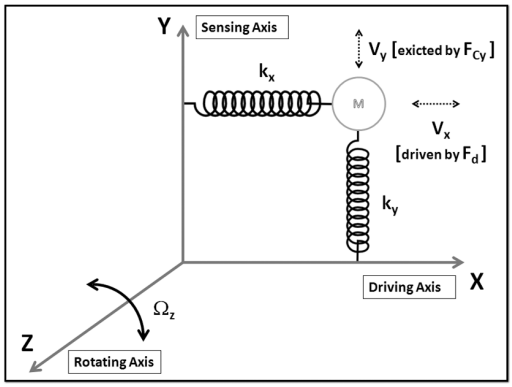

Figure 1: Schematic diagram of a vibratory gyroscope system. An internal driving force induces the spring-mass system to vibrate in one direction, the x-axis in this example. An external rotating force, perpendicular to the xy-plane induces oscillations in the y-direction by transferring energy through the Coriolis force. These latter oscillations can be used to detect and quantify the rate of rotation.

Normally a higher amplitude response of the y-axis translates to an increase in sensitivity of a gyroscope. Thus, to achieve high sensitivity most gyroscopes operate at resonance in both drive- and sense-modes. But since the phase and frequency of the sense-mode is determined by the phase and frequency of the Coriolis force which itself depends on those of the driving signal, most gyroscopes operate exactly at the drive-mode resonant frequency while

the sense-mode frequency is controlled to match the drive-mode resonant frequency. Consequently, the performance, in terms of accuracy and sensitivity, of a gyroscope depends greatly on the ability of the driving signal to produce stable oscillations with constant amplitude, phase, and frequency. To achieve these important requirements, a variety of schemes, based mainly on closed-loops and phase-locked loops circuits, have been proposed [18]. Recently parametrical resonance in MEMS (Micro-Electro-Mechanical Systems) gyroscopes has also been extensively studied as an alternative to harmonically driven oscillators. In this work we consider an alternative approach to increase performance based on a weakly coupled network. The *fundamental idea* is to synchronize the motion of each gyroscope to the Coriolis driving force, so that the collective signal from all gyroscopes can be summed and then demodulated to yield an optimal response in terms of minimizing phase drift and robustness to noise and material imperfections.

2. Modeling

Based on the fundamental principles of operation illustrated in Figure 1, the governing equations of a bidirectionally coupled ring of gyroscopes is described by the following system of differential equations

$$\begin{aligned} m\ddot{x}_i + c_x\dot{x}_i + \kappa_x x_i + \mu x_i^3 &= f_e(t) + 2m_i\Omega\dot{y}_i + \\ &\quad \lambda_{ij}(x_{i+1} - 2x_i + x_{i-1}) \\ m\ddot{y}_i + c_y\dot{y}_i + \kappa_y y_i + \mu y_i^3 &= -2m_i\Omega\dot{x}_i, \end{aligned} \tag{1}$$

where x (y) represents the drive (sense) modes, m is the proof mass, Ω_z is the angular rate of rotation along a perpendicular direction (z-axis), c_x (c_y) is the damping coefficient along the x- (y-) direction, and κ_x (κ_y) and μ_x (μ_y) are the linear and nonlinear damping coefficients along the x- (y-) directions, respectively, $i \sim j$ denotes all the j^{th} gyroscopes that are coupled to the i^{th} gyroscope, λ_{ij} denotes the coupling strength, and $f_e(t) = A_d \sin\omega_d t$ the sinusoidal driving force with amplitude A_d and frequency ω_d.

2.1. Hamiltonian Formulation

Let $q_i = (q_{i1}, q_{i2})^T = (x_i, y_i)^T$ be the configuration components and $p_i = m\dot{q}_i + Gq_i$ be the momentum components of a single gyroscope, where

$$G = \begin{pmatrix} 0 & -m\Omega \\ m\Omega & 0 \end{pmatrix}.$$

Directly differentiating the momentum components, we get (after rearranging terms) $m\ddot{q}_i = \dot{p}_i - G\dot{q}_i$. Then the original equations (1), which have total phase space $\mathbf{R}^{4N}$, can be written in the following form. Letting $Z_i = (q_i, p_i)$, the internal dynamics of each individual i^{th} gyroscope can be expressed as follows

$$\mathcal{F}(Z_i) = \begin{pmatrix} -\frac{G}{m} & \frac{1}{m}I_2 \\ -\frac{GF}{m} + K - \frac{1}{m}G^2) & \frac{1}{m}(F - G) \end{pmatrix}\begin{pmatrix} q_i \\ p_i \end{pmatrix} + \begin{pmatrix} 0 \\ -f_i \end{pmatrix},$$

with $F = \mathrm{diag}(c_x, c_y)$, $K = \mathrm{diag}(\kappa_x, \kappa_y)$ and $f_i = \mu(q_{i1}^3, q_{i2}^3)^T$. Then the governing equations of the $\mathbf{D}_N$ symmetric ring can be written as in (**??**), that is

$$\frac{dZ_i}{dt} = \mathcal{F}(Z_i) + \mathcal{H}(Z_{i+1}, Z_i) + \mathcal{H}(Z_{i-1}, Z_i) + R(t), \tag{2}$$

where $R(t) = (0, f_e(t), 0, 0)^T$,

$$\mathcal{H}(Z_{i+1}, Z_i) = \begin{pmatrix} 0 \\ \lambda\Gamma(q_{i+1} - q_i) \end{pmatrix} \quad \text{and} \quad \Gamma = \begin{pmatrix} 1 & 0 \\ 0 & 0 \end{pmatrix}.$$

Since the nonlinear terms are given only by cubic terms each gyroscope is symmetric with respect to the $-I$ transformation $(q_i, p_i) \to (-q_i, -p_i)$. Because the coupling is also symmetric with respect to this $\mathbf{Z}_2(-I)$-symmetry; that is, $\mathcal{H}(-Z_{i+1}, -Z_i) = -\mathcal{H}(Z_{i+1}, Z_i)$, then the networks have symmetry group given by $\mathbf{D}_N(\gamma, \eta) \times \mathbf{Z}_2(-I)$.

For the remainder of this section we assume $c_x = c_y = 0$ and consider the unforced systems with $f_e = 0$. Later on we discuss the effects of damping and the periodic driving signal as well. Direct calculations show that the network equations (2) are Hamiltonian and can be expressed in terms of position and momentum coordinates $(q, p) = (q_1, \ldots, q_N, p_1, \ldots, p_N)$ as

$$\begin{aligned} H(q,p) = \frac{1}{2}\sum_{i=1}^{N} -p_i^T\left(K - \frac{G^2}{m} + 2\lambda\Gamma\right)q_i - q_i^T\frac{G}{m}q_i + \\ p_i^T\frac{G}{m}p_i + q_i^T\frac{I_2}{m}p_i - (q_{i+1} + q_{i-1})^T\lambda\Gamma q_i + H_2(q,p), \end{aligned} \tag{3}$$

3. Main Results

In this section we state the main results of the effects of the main bifurcation parameter, the coupling strength λ, and the forcing (recall that in the previous section we have assumed $f_e(t) = 0$) on the network dynamics. We show that existence and stability of periodic solutions of the forced system, $f_e(t) \neq 0$, are in one-to-one correspondence with those of the equilibrium solutions of the unforced system, $f_e(t) = 0$. Furthermore, we state one of the main results of this manuscript: a theorem that provides an analytic expression for the onset, as λ is varied, of fully synchronized periodic solutions which preserves the $\mathbf{D}_N \times \mathbf{Z}_2$–symmetry of the ring and that is valid for any ring size N. This is the expression that was very difficult to obtain through perturbation methods [**?**, **?**]

3.1. Synchronized Periodic Solution

We consider again the governing equations for the bidirectional ring (without forcing) written as a separation of linear M and nonlinear terms, that is

$$\frac{dZ}{dt} = MZ + F(Z), \tag{4}$$

where again: $Z = (Z_1, \ldots, Z_N)^T$, $Z_i = (q_i, p_i)^T$, $F = (F_1, \ldots, F_N)^T$, and $F_i = (0, -f_i)^T$ with $i = 1, \ldots N$ mod

N. Also, recall that $M = M_{bi}$. Let $\tau = t$ and now write the system in extended phase space

$$\frac{dZ}{dt} = MZ + F(Z) + H_A(\tau) := S(Z, \tau, A), \qquad \frac{d\tau}{dt} = 1. \quad (5)$$

where

$$H_A(\tau) = \underbrace{(0, f_e(\tau), 0, 0, \ldots, 0, f_e(\tau), 0, 0)}_{N \text{ times}}.$$

We can now state one important result, which includes an analytical expression for the onset of synchronized solution in the forced-driven gyroscope with no damping. The effects of small damping are discussed at the end of this section. We make the following assumption for the remainder of the paper:

$$\kappa_x = \kappa_y =: \kappa.$$

Recall that an equilibrium is *spectrally stable* if all the eigenvalues of the linearization of the equilibrium are on the imaginary axis and for a periodic orbit, if all its Floquet multipliers are on the unit circle. A stronger concept for the system obtained from linearization near equilibrium or periodic orbit is *strong stability* also called *parametric stability*. A linear periodic Hamiltonian system is strongly stable if all solutions are bounded for all $t \in \mathbf{R}$ and the same remains true for sufficiently small linear Hamiltonian periodic perturbations, see [**?**]. Note that strong stability implies spectral stability.

Theorem 3.1 *If the forcing parameter A is small enough, system (5) with bidirectional coupling has a fully synchronized $2\pi/\omega$-periodic solution $\tilde{Z}(t)$ near Z_0 with isotropy subgroup $\mathbf{D}_N \times \mathbf{Z}_2$, strongly stable for*

$$\lambda > \lambda^* = -\frac{\kappa}{2(1 - \cos(2\pi\lfloor N/2 \rfloor / N))}. \quad (6)$$

The proof of this theorem is done in several steps. In the following proposition, we begin by establishing the relationship between equilibrium solutions of the unforced system with periodic solutions of the forced system with small coupling parameter A.

Proposition 3.2 *For the forcing frequency $\omega \in \mathbf{R} \setminus \{$a finite number of points$\}$, equilibrium solutions of the unforced system (4) are in one-to-one correspondence with $2\pi/\omega$-periodic solutions of (5). Moreover,*

1. *If Z_0 is an equilibrium solution of (4) with isotropy subgroup Σ, then the corresponding periodic solution $P_0(t)$ has spatial isotropy subgroup Σ.*

2. *Z_0 is spectrally stable/strongly stable/unstable if and only if $P_0(t)$ is spectrally stable/strongly stable/unstable.*

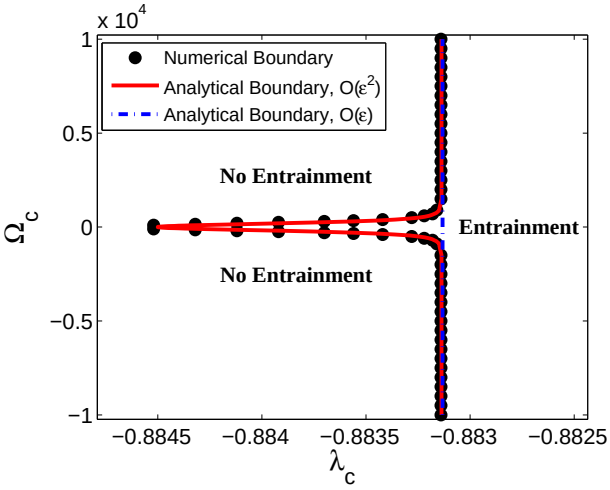

Figure 2: Two-parameter bifurcation diagram outlines the region of parameter space (Ω, λ) where the vibrations of a system of three gyroscopes, coupled bi-directionally, become completely synchronized. The boundary curve corresponds to the locus of the pitchfork bifurcation where three periodic solutions of the motion equations (5) merge into a $\mathbf{D}_3 \times \mathbf{Z}_2$ symmetric one as the complete synchronization state becomes locally asymptotically stable.

Observe that for the special case of a ring with $N = 3$ gyroscopes, Eq. (6) yields $\lambda^* = -\kappa/3$. Based on parameter values estimated experimentally, we set $\kappa = 2.6494$ N/meter to get $\lambda^* = -0.8831$. This value fits very well the almost vertical line threshold, in parameter space (Ω, λ), which was originally obtained through asymptotic methods [**?**] , and reproduced in Fig. 2. The only difference is the cusp shape, which is due to the effects of damping. Recall that damping has been neglected in our analysis in order to preserve the Hamiltonian structure of the cells and of the network. Nevertheless, that cusp region is extremely small considering the scale along the λ-axis.

Our last result is concerned with the bifurcating solutions from the $2\pi/\omega$-periodic solution $\tilde{Z}(t)$ as the coupling parameter decreases below λ^*.

Theorem 3.3 *A $\mathbf{Z}_2(-I)$-orbit of branches of periodic solutions $\tilde{Z}^b(t)$ with isotropy subgroup $\mathbf{Z}_2(\kappa)$ bifurcates from $\tilde{Z}(t)$ as λ decreases below λ^*. For N odd, the $\mathbf{Z}_2(\kappa)$ orbit has a form conjugate to*

$$\tilde{Z}^b(t) = (Z_1^b(t), Z_2^b(t), \ldots, Z_N^b(t)),$$

with $Z_j^b(t) = Z_{N+2-j}^b(t)$ for $j = 2, \ldots, (N+1)/2$. For N even, $\tilde{Z}^b(t)$ satisfies a form conjugate to the conditions $Z_j^b(t) = Z_{\frac{N}{2}+j}^b(t)$ for $j = 1, \ldots, N/2$.

The proof of this theorem is done by showing the existence of a pitchfork bifurcation from the synchronous equilibrium solution in the non-forced system.

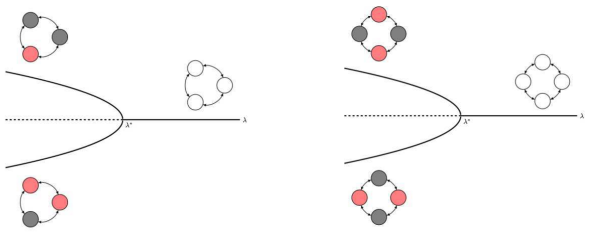

Figure 3: Diagrams illustrating the bifurcation of the strongly stable synchronized solution to synchrony-broken patterns with $\mathbf{Z}_2(\kappa)$-symmetry when λ decreases below λ^* as described by Theorems 3.1 and 3.3. This bifurcation comes from a pitchfork bifurcation of the unforced system and is illustrated via the diagram. The shades of grey in the circles identify the synchronized gyroscopes.

Figure 3 illustrates the results of Theorem 3.1 and Theorem 3.3 for the cases $n = 3$ and $n = 4$. The synchronized periodic solution is strongly stable for $\lambda > \lambda^*$, loses its stability at $\lambda = \lambda^*$ and bifurcates to $\mathbf{Z}_2(\kappa)$-symmetric periodic solutions for $\lambda < \lambda^*$. Because this transition comes from a pitchfork bifurcation of the unforced system, the $-I$ symmetry relates the two bifurcating solutions. The shades of grey (or colours) identify the synchronized gyroscopes.

Acknowledgments

B.S.C. and A.P. were supported by the Complex Dynamics and Systems Program of the Army Research Office, supervised by Dr. Samuel Stanton, grant W911NF-07-R-003-4. A.P. was also supported by the ONR Summer Faculty Research Program, at SPAWAR Systems Center, San Diego. V.I. acknowledges support from the Office of Naval Research, Code 30 managed by Dr. Michael F. Shlesinger. P-L.B. acknowledges the funding support from NSERC (Canada) in the form of a Discovery Grant.

References

[1] M.E. Tuckerman, B.J. Berne, and G.J. Martyna. Molecular dynamics algorithm for multiple time scales: systems with long range forces. *J. Chem. Phys.*, 94(10):6811–6815, 1991.

[2] N.E. Leonard and J.E. Marsden. Stability and drift of underwater vehicle dynamics: Mechanical systems with rigid motion symmetry. *Physica D*, 105(1-3):130–162, June 1997.

[3] A. Bulsara, V In, A. Kho, A. Palacios, P. Longhini, S. Baglio, and B. Ando. Exploiting nonlinear dynamics in a coupled core fluxgate magnetometer. *Measurement Science and Technology*, 19:075203, 2008.

[4] V. In, A. Palacios, A. Bulsara, P. Longhini, A. Kho, Joseph Neff, Salvatore Baglio, and Bruno Ando. Complex behavior in driven unidirectionally coupled overdamped duffing elements. *Physical Review E*, 73(6):066121, 2006.

[5] A. Palacios, J. Aven, P. Longhini, V. In, and A. Bulsara. Cooperative dynamics in coupled noisy dynamical systems near a critical point; the dc squid as a case study. *Physical Review E*, 74:021122, 2006.

[6] C. Acar and A.M. Shkel. *MEMS Vibratory Gyroscopes: Structural Approaches to Improve Robustness*. Springer, 2009.

[7] N. Sri Namachchivaya and W. Nagata. Bifurcations in gyroscopic systems with an application to rotating shafts. *Proc. R. Soc. Lond. A*, 454:543–585, 1998.

[8] M.S. Grewal, L.R. Weill, and A.P. Andrews. *Global POsitioning Systems, Inertial Navigation, and Integration*. Wiley-Interscience, 2007.

[9] R. Rogers. *Applied Mathematics in Integrated Navigation Systems*. American Institute of Aeronautics and Astronautics, 2007.

[10] R.J. McDonald, N. Sri Namachchivaya, and W. Nagata. Bifurcations of gyroscopic systems near a 0 : 1 resonance. *Fileds Institute Communications*, 49:79–116, 2006.

[11] L. Kocarev and G. Vattay. *Complex Dynamics in Communication Networks*. Springer, New York, 2005.

[12] Y. Susuki, Y. Takatsuji, and T. Hikihara. Hybrid model for cascading outage in a power system: A numerical study. *IEICE Trans. Fundamentals*, E92-A(3):871–879, 2009.

[13] M. Golubitsky, I. Stewart, and D.G. Schaeffer. *Singularities and groups in bifurcation theory*, volume 2. Springer–Verlag, New York, 1988.

[14] CH. Skokos. On the stability of periodic orbits of high dimensional autonomous hamiltonian systems. *Physica D*, 159(3-4):155–179, November 2001.

[15] P. Smereka. Synchronization and relaxation for a class of globally coupled hamiltonian systems. *Physica D*, 124(1-3):104–125, December 1998.

[16] V. Apostolyuk. *MEMS/NEMS Handbook*, volume 1. Springer, 2006.

[17] V. Apostolyuk and F. Tay. Dynamics of michromechanical coriolis vibratory gyroscopes. *Sensor Letters*, 2:252–259, 2004.

[18] A.M. Shkel. Type i and type ii micromachined vibratory gyroscopes. In *Proceedings IEEE/ION PLANS*, pages 586–593, San Diego, CA, 2006.